The importance of observation of structural changes of lead acid battery active mass in special applications in the mining industry

***Jana Zimáková*[1], *Sebastian Vaculík*[1], *Petr Bača*[1] *and* *Daniel Fryda*[1]**

To be able to use lead acid batteries in particularly difficult conditions in the mining industry, it is very important to understand the events that occur during traction operation of mining carts, or auxiliary lighting. Failure of lead accumulators in the hazardous environments, where it is desired non-explosive embodiment, may have fatal consequences. The paper describes the possibility of observing changes in active materials at the microscopic level.

The process of charging and discharging lead-acid accumulator has been described in many publications. The aim of this article is to supplement known information about a series of images and analysis that will accurately show progressive changes in the structure of the negative electrode. Negative electrodes are, at each cycle, charged and discharged under the same conditions, scanned with a scanning electron microscope, the elemental analysis (EDS) is performed, and the size of the individual sulfate crystals is measured. Previously measured results indicate that during the charging the conversion of $PbSO_4$ crystals into a charged form of the active mass is not complete, and there is a rapid increase in the size of lead sulfate crystals on the negative electrode. This article compares changes in electrode surface composition after two cycles. There is a clear loss of lead and, on the other hand, the visible growth of sulfur. This indicates progressive surface sulfation.

***Key words**: atomic force microscopy, environmental scanning electron microscopy, negative active mass, lead-acid accumulator*

Introduction

Lead acid batteries were invented in 1859 by Gaston Planté and first demonstrated to the French Academy of Sciences in 1860. Even after so many years since its invention, improvements are still being made to the lead acid battery and despite its shortcomings and the competition from newer cell chemistries; the lead acid battery still retains the lion's share of the high power battery market [13]. Despite their high weight and relatively low durability (compared to other systems), they are, due to their low-cost valuable, high reliability, and recyclability, irreplaceable in many application areas. One of the application areas is mining.

Mining is one of the most demanding environments and coal miners know that safe, reliable equipment is critical to their operation [14]. Underground mines require unique vehicles (figure 1b) with low profiles and no carbon emissions. A mining battery (figure 1a), also known as a traction battery, comprises of some 2 V individual cells that are connected in series by means of copper cable connectors to form a certain voltage to give power to the required application [13].

a) **b)**

Fig. 1. Examples of using the lead acid battery in mining: a) mining battery, b) vehicles [13].

To tackle energy and environmental issues, many companies and institutions deals with the development of electric vehicles (EV), hybrid electric vehicles (HEV), systems for load balancing (load leveling systems - LL) and other devices. It can be assumed that mainly lead-acid accumulators will be used to power these systems.

[1] *Ing. Jana Zimáková, Ing. Sebastian Vaculík, doc. Ing. Petr Bača, Ph.D., Ing. Daniel Fryda,* The Faculty of Electrical Engineering and Communication, Brno University of Technology, Department of Electrotechnology, xzimak00@stud.feec.vutbr.cz

However, the key properties (especially performance and durability) of the accumulators are often inadequate for these purposes. Therefore, it is necessary to perform the analysis of chemical reactions on active mass. After that, we should be able to explain processes occurring at the electrodes in detail and propose new batteries with better performance properties.

Only a few research groups in the world are dedicated to in situ observation of processes on the lead acid accumulator electrodes. The most significant results were achieved by scientists from the Department of Materials Science at Osaka University, in collaboration with Yuasa Corporation. The following analyzes were performed: reactions on the surface of the lead electrodes in an aqueous solution of sulfuric acid [1-3], in situ observation of sulfate crystals growth while charging [4, 5], and it was also studied the influence of additives on the final properties [6-9]. An electron microscopy (SEM) and cyclic voltammetry (CV) in combination with an electrochemical atomic force microscopy (EC-AFM) was used for the analysis and measurement.

Experiment

The aim of the experiment described below was monitoring changes in the surface structure of the negative electrode during their cycling. For this purpose, it was necessary to build an experimental cell consisting of the negative electrode, which has been the subject of investigation, and the counter electrode. Both of these electrodes were made up by lead profiles, a mercurous sulfate electrode (Hg / Hg_2SO_4, K_2SO_4, c = sat.) was chosen as a reference electrode.

In the first stage of the experiment, it was necessary to create a thin layer of $PbSO_4$ on the surface of the negative electrode. Due to the characteristics of lead resulting from the Pourbaix diagram shown in Figure 2 and by using mercurous sulfate electrode with the potential of E0 = 640 mV vs. NHE, this layer was accomplished by immersing the lead profiles in a weak aqueous solution of H_2SO_4 with pH = 2 and then held at zero potential vs. NHE for 30 minutes. A VSP potentiostat with control software ECLab v. 10.33 was used as a measuring instrument.

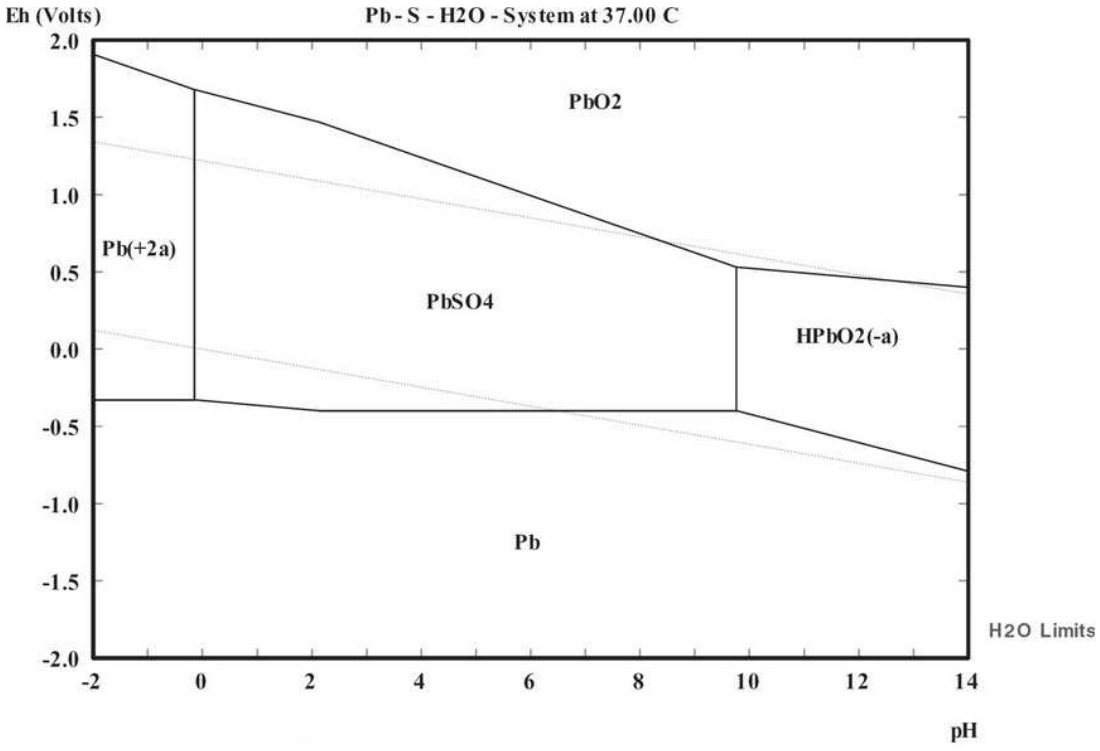

Fig. 2. Potential-pH diagram of lead in the presence of sulfate ions at unit activity [10].

After 1,5h, the electrode surface was scanned by using an environmental scanning electron microscope Tescan VEGA 3 XM equipped with X-ray detectors from Bruker - XFlash 6|10 for elemental analysis of samples and by an atomic force microscope (AFM - Agilent 5500 SPM). Before measuring, it was necessary to rid lead profiles of sulfuric acid residues. Otherwise, it could cause irreversible damage to ESEM. Therefore, electrodes were immersed in several baths of deionized water before the scanning. The surface structure of the negative electrode after this part of the experiment is shown in Figure 3.

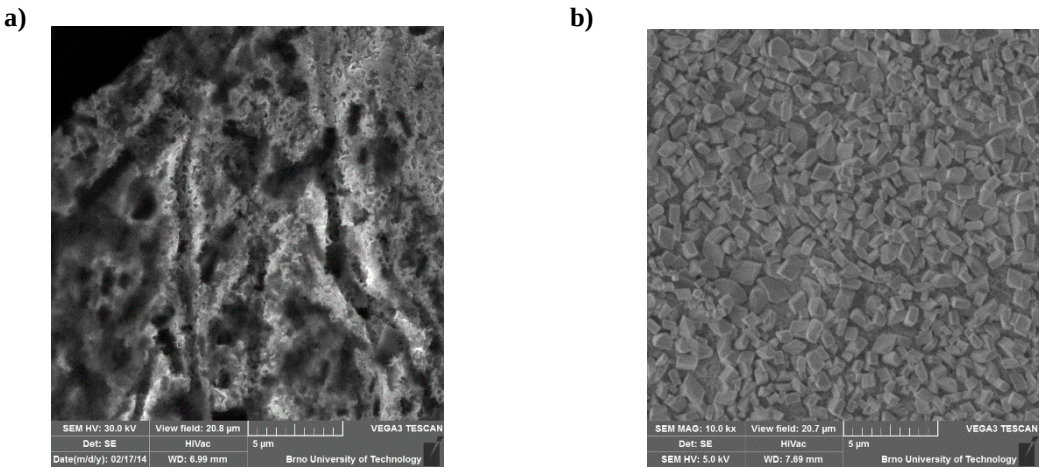

Fig. 3. Microscopic structure of the electrode surface - a) the original lead profile (ESEM); b) $PbSO_4$ crystals (ESEM).

In the second stage of the experiment, two experimental cells were compiled, in which the working electrode was formed by the negative lead profiles, whose surface was covered with a thin layer of $PbSO_4$, a pure lead was used as the counter electrode (Fig. 4). These cells were subsequently cycled. After each charging and discharging, the negative electrode was rinsed in several baths of deionized water and scanned by using the above-described ESEM. AFM has not been used in this case because the size of the crystals did not allow it.

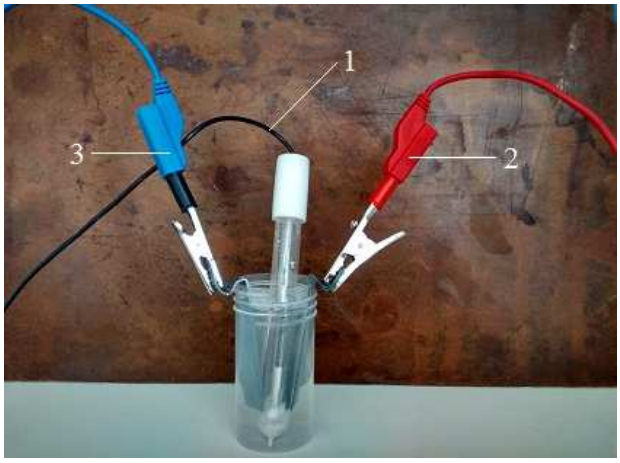

Fig. 4. Experimental cell – 1) mercurous sulfate referent electrode, 2) counter electrode, 3) negative electrode (lead profile).

Charging was carried out galvanostatically with the current of -1 mA up to the final voltage of -1,026 V vs. MSRE. This electrode potential was maintained for 45 minutes. Discharging was also performed galvanostatically with the current of 0,5 mA to the final voltage of -0,4 V vs. MSRE. After that, it was held at this potential for 45 another minutes. Two cycles were carried out. Chemical reactions occurring during this cycling are described by the following equation:

$$2PbSO_4 + 2H_2O \leftrightarrow PbO_2 + 2H_2SO_4 + Pb$$

(right arrow indicates the direction of reaction during charging and left arrow while discharging)

Discharging leads to the transformation of the electrode's active mass on the lead sulfate ($PbSO_4$). The electrolyte is sapped of its sulfuric acid (H_2SO_4) and enriched with water. The concentration of the sulfuric acid decreases. Charging creates sulfuric acid, and the electrolyte becomes denser. At the end of charging, a dark brown lead dioxide (PbO_2) is found at the surface of the positive electrode and a dark gray sponge lead on the negative electrode [11].

The surface of the electrode in the charged and discharged state is shown in Figures 4 and 5.

a) **b)**

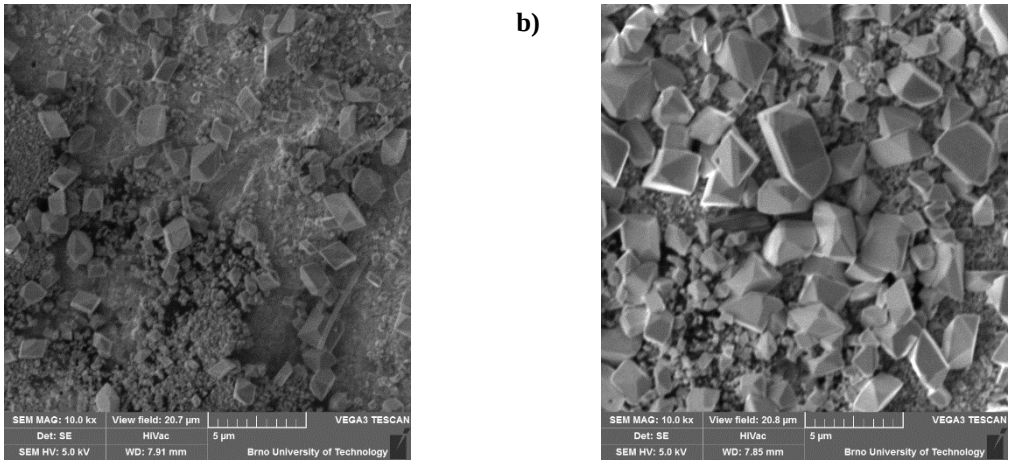

Fig. 5. Microscopic structure of the electrode surfaces (first cycle) - a) charged state; b) discharged state.

a) **b)**

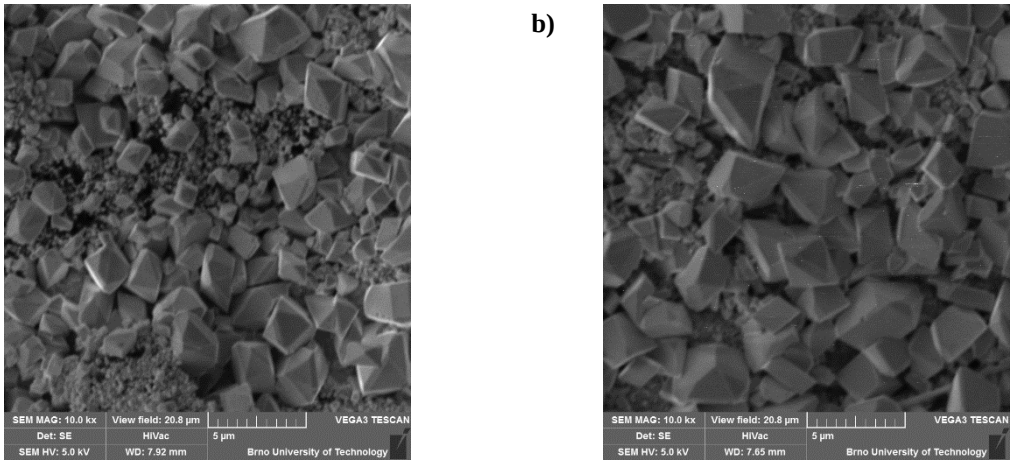

Fig. 6. Microscopic structure of the electrode surfaces (second cycle) - a) charged state; b) discharged state.

While discharging, electrodes were covered with poorly soluble lead sulfate that had, in comparison with lead oxide and lead dioxide, very low conductivity (less than 10^{-8} Scm^{-1} versus $4{,}8x10^{6}$ Sm^{-1} with lead [12]). This low conductivity complicated observation. In the final pictures, it was shown as bright crystal edges where the electric charge of the electron beam was accumulated.

Results

To be able to use lead acid batteries in particularly difficult conditions in the mining industry, it is very important to understand the events that occur during traction operation of mining carts, or auxiliary lighting. Failure of lead accumulators in the hazardous environments, where a nonexplosive embodiment is desired, may have fatal consequences. Therefore, it is an important observation of changes in active mass at the microscopic level and detailed understanding of the mechanisms of these processes and their subsequent modifications.

Formation of lead sulfate crystals, at the beginning of the experiment (Fig. 3), was as anticipated. Formed $PbSO_4$ crystals were homogeneously distributed over the entire surface of the electrode. The size of the most of formed crystals was below 1µm. A few formed crystals had a size greater than 2µm. After charging (Fig. 5a), sulfate crystals were transformed, and a layer of highly porous sponge lead was formed. However, it is evident that the charging process has been particularly effective in small sulfate crystals. While the charging process did not proceed with sufficient efficiency for crystals larger than about 2µm - these large sulfate crystals remained unchanged at the end of charging. This created inhomogeneous structure. After discharging (Fig. 5b), the existing sulfate crystals grew larger and only a few new crystals were created. Inhomogeneity continues to grow, both fungal lead and sulfate crystals in sizes ranging from tenths microns to about five microns can be observed in the image. The findings above are shown even in the second cycle - Figure 6a, 6b. It can be summarized that the conversion of all sulfate was not effective while charging, this process was difficult especially for large crystals. With each carried cycle, the size of individual crystals gradually expanded.

This illustrates the progressive sulfation, thus re-crystallization processes leading to the growth of the crystal, creating the insulating layer of nonconductive poorly soluble sulfates and deterioration of charging ability of the electrode.

This is demonstrated by data obtained by measuring the sizes of randomly selected lead sulfate crystals. Measuring was performed by using of evaluation software of the microscope Tescan Vega (Fig. 7). The results of this measurements are shown in Table 1.

The results of the elemental analysis performed after each cycle are presented in Table 2.

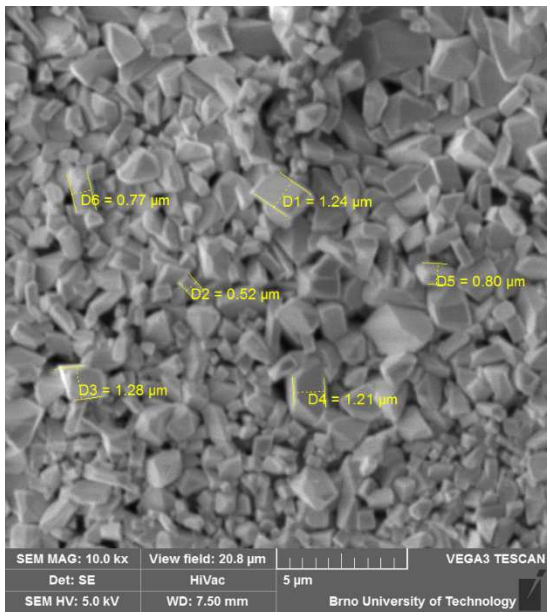

Fig. 7. Microscopic structure of the electrode surfaces – measuring of sulfate crystal's sizes.

Tab. 1. Measured size of lead sulfate crystals in [µm] during each cycle.

	1. electrode					**2. electrode**				
Measurement No.		**1 cycle**		**2 cycle**			**1 cycle**		**2 cycle**	
	After formation [µm]	After charging [µm]	After dis-charging [µm]	After charging [µm]	After dis-charging [µm]	After formation [µm]	After charging [µm]	After dis-charging [µm]	After charging [µm]	After dis-charging [µm]
1	0,53	1,35	3,25	2,18	3,20	0,58	1,23	1,22	1,24	1,70
2	0,73	1,12	2,02	1,72	2,20	0,34	0,90	0,63	1,21	1,51
3	0,86	1,10	2,21	1,81	2,43	0,35	0,43	0,53	1,28	1,25
4	1,25	0,66	1,57	2,65	2,84	0,60	0,64	1,06	0,80	0,72
5	1,48	0,83	1,42	1,62	1,91	0,80	0,45	0,94	0,77	0,75
ϕ	0,97	1,01	2,09	2,00	2,52	0,53	0,73	0,88	1,06	1,19

Tab. 2. Distribution of chemical elements in the negative electrode during each cycle.

		element	norm. C [wt.%]	sigma [wt.%]
1st cycle	charged	Sulfur	2,18	0,28
		Lead	83,59	5,1
	discharged	Sulfur	9,63	0,8
		Lead	55,72	2,85
2nd cycle	charged	Sulfur	8,22	0,74
		Lead	62,63	3,45
	discharged	Sulfur	11,2	1,11
		Lead	77,22	4,77

Conclusion

During the charging and discharging, the surface of lead-acid battery electrodes is covered with a layer of sulphates. The aim of our work is in situ observation of morphology changes on electrodes.

The figures show that charging is not fully reversible reaction, a certain amount of sulphate crystals does not turn into sponge lead. The amount of sulfate crystals in the charged state is increasing, their incorporation into the structure of sponge lead is evident. Sulfate crystals are gradually increasing. This indicates a progressive sulphation, i.e. the re-crystallization processes leading to crystal growth and deterioration of the charging ability of the electrode. This is also confirmed by the values shown in Table 1, which lists the crystal's sizes measured on 2 investigated negative electrodes.

The experiment is still ongoing, and, therefore, the results are not complete. The results will be published in following works.

Acknowledgment: *This research work has been carried out in the Centre for Research and Utilization of Renewable Energy (CVVOZE). Authors gratefully acknowledge financial support from the Ministry of Education, Youth and Sports of the Czech Republic under NPU I program (Project No. LO1210).*

References

[1] Yamaguchi Y., Shiota M., Nakayama Y., Hirai N., Hara S.: In situ analysis of electrochemical reactions at a lead surface in sulfuric acid solution. *Journal of Power sources. 2000, vol. 85, p. 22 – 28. ISSN: 0378 7753*

[2] Yamaguchi Y., Shiota M., Nakayama Y., Hirai N., Hara S: Combined is situ EC-AFM and CV measurement study on lead electrode for lead-acid batteries. *Journal of Power sources. 2001, vol. 93, p. 104 - 111*

[3] Shiota M., Yamaguchi Y., Nakayama Y., Adachi K., Taniguchi S., Hirai N., Hara S.: In situ observation of morphology change in lead dioxide surface for lead-acid battery. *Journal of Power sources. 2001, vol. 95, p. 203-208. ISSN: 0378-7753*

[4] Yamaguchi Y., Shiota M., Hosokawa M., Nakayama Y., Hirai N., Hara S.: Study of chargé acceptance for the lead-acid battery trough in situ EC-AFM observation – influence of the open-circuit standing time on negative electrode. *Journal of Power sources. 2001, vol. 101, p. 155-161*

[5] Hirai N., Kubo S., Magara K.: Combined cyclic voltammetry and in situ electrochemical atomic force microscopy on lead electrode in sulfuric acid solution with or without lignosulfonate. *Journal of Power sources. 2009, vol. 191, p. 97 – 102*

[6] Ban I., Yamaguchi Y., Nakayama Y., Hirai N., Hara S.: In situ EC-AFM study of effect of lignin on performance of negative electrodes in lead-acid batteries. *Journal of Power sources. 2002, vol. 107, p. 167 - 172*

[7] Hirai N., Tabayashi D., Shiota M., Tanaka T.: In situ electrochemical atomic force microscopy of lead electrodes in sulfuric acid solution with or without lignin during anodic oxidation and cathodic reduction. *Journal of Power sources, 2004, vol. 133, p. 32 – 38*

[8] Miyake M., Morikawa H., Minato I., Iwai S-I.: Am. Mineralogist 1978, *vol. 63, p. 506 – 510*

[9] Vernesan H., Hirai N., Shiota M., Tanaka T.. Effect of barium sulfate and stroncium sulfate on charging and discharging of the negative electrode in a lead-acid battery. *Journal of Power sources, 2004, vol. 133, p. 52 – 58*

[10] *Available at* http://www.oocities.org/capecanaveral/campus/5361/chlorate/leaddiox/alfabeta.html

[11] Pavlov, D. Lead-acid batteries: Science and technology, A handbook of lead-acid battery technology and its influence on the product, *Elsevier, 2011*

[12] *Available at* http://www.tibtech.com/conductivity.php

[13] *Available at* http://www.battery.co.za/products/mining/

[14] *Available at* http://www.douglasbattery.com/default.aspx?id=63